COMPACT X-BAND LINEAR ACCELERATORS DESIGN FOR ON-SITE INDUSTRIAL APPLICATIONS*

M. Boucard†, AVELION, Peynier, France
Y. Rozier, Epsyl, Pertuis, France

Abstract

The progressive replacement of radioactive sources is stimulating growing interest in compact linear accelerators, which are better suited for field deployment. Such systems must emphasize modularity, transportability, and, above all, reliable performance under operational conditions.

This work introduces a family of compact X-band linear accelerators designed to produce electron beams in the low-MeV energy. The engineering design focuses on the key component: the accelerating structure. A biperiodic on-axis coupled standing-wave structure was selected, operating in $\pi/2$ mode.

Simulation results demonstrate that the proposed configurations achieve the targeted energy levels with controlled beam transmission, while providing a focal spot size (FWHM) below 1 mm, significantly outperforming conventional radioactive sources ($\approx$ 5 mm).

This paper summarizes the overall design approach, highlights the main simulation results, and outlines the current progress of development activities.

INTRODUCTION

Among the various methods of non-destructive testing (NDT), X-ray imaging plays a key role, particularly for the inspection of thick materials. Currently, on-site NDT applications rely mainly on radioactive sources such as ^{60}Co and ^{192}Ir. However, these sources present several limitations, including their relatively low dose rates, stringent regulatory constraints associated with their handling and storage, and the fact that they continuously emit radiation even when not in operation [1].

Linear accelerators offer a promising alternative as they can generate X-rays with sufficiently high energy to penetrate thick materials structures, along with dose rates that enable rapid radiographic [2].

Despite these advantages, their use in NDT is usually reserved for controlled environments such as bunkers. The purpose of the system under development is to replace radioactive sources for on-site industrial applications [3]. The system must combine several key requirements, including transportability, modularity, simplicity, and reliability.

NDT linear accelerators typically work in S-band (3 GHz). Increasing the resonant frequency of the accelerating structure offers the possibility to scale down overall dimension of the system. An answer to this requirement could be found at upper frequencies in the X-band.

* This work was supported by a grant from the French Public Investment Bank (Bpifrance) as part of the France 2030 program.
† mboucard@avelion-alcen.com

Operation in the X-band is advantageous not only for reducing the system dimensions but also for improving the nominal performance. For the same radio-frequency (RF) power, for example, higher beam energies can be achieved. In addition, the filling time is reduced, the shunt impedance is increased, and a higher maximum electrical field strength can be obtained [4].

The purpose of this work is to design an X-band accelerating structure that satisfies the associated space constraints. This paper outlines the main design choices along with the results obtained from RF modeling and beam dynamics simulations.

ACCELERATING STRUCTURE DESIGN

Product Specifications

To achieve the objective of modularity and transportability, the accelerating structure should fulfill specific requirements, especially in terms of length and accelerating gradient. However, these constraints should not compromise the beam quality in term of current, transmission, energy, and spot size. The chosen frequency band is the X-band, around 9.3 GHz, with a magnetron pass band ranging between 9.275 GHz and 9.315 GHz. The RF power delivered by the magnetron can be up to 1.75 MW peak. The resulting specifications are summarized in Table 1. The target energy of 1.8 MeV has been selected as the most effective level for replacing the radioactive sources.

Table 1: Specifications of the X-band Accelerator

Item	**Value**	**Unit**
Energy	1.8	MeV
Transmission	> 30 %	
Quality factor	> 8000	
Shunt impedance	> 150	MΩ/m
Frequency	9.275 to 9.315	GHz
Beam spot size (FWHM)	< 1	mm
On-axis peak gradient	> 40	MV/m
Peak RF input power	< 1.75	MW

Design

The selected design is a bi-periodic on-axis coupled standing wave structure.

The mode $\pi/2$ is chosen due to its favorable characteristics on the dispersion curve. The coupling cells are located on the axis, which helps reduce the overall diameter and has a minimal effect on the total length of the system. Moreover, this kind of design builds upon previous accelerators developed by AVELION.

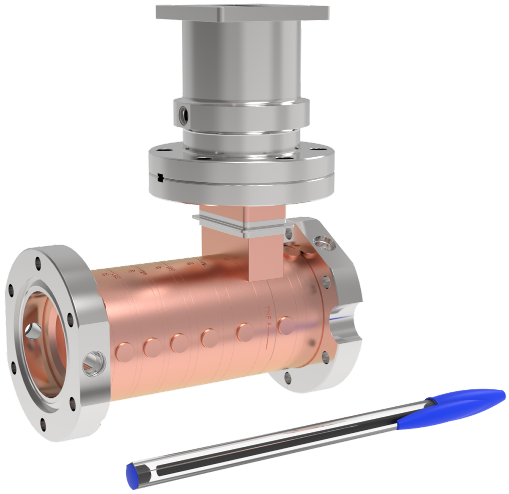

Figure 1: Accelerating structure mechanical design.

The accelerating structure consists of a 4-cavity buncher, followed by a series of relativistic cavities depending on the target energy. For a beam energy of 1.8 MeV, 7 accelerating cavities are required, resulting in a total length of less than 10 cm.

The profile of the inside of the cavity: the noses, the gap between the noses, the aperture, the coupling holes, the thickness of the wall, have been determined using a design of experiments approach. The objective was to maximize the shunt impedance while minimizing the fields on the surface. Figure 1 shows the final design of the 1.8 MeV accelerating structure including the RF window, which is also under development [5]. The shape of the taper which couples the RF window to the accelerating structure has been determined to maximize coupling efficiency while minimizing length, consistent with the objective of reducing the overall footprint. The frequency of each cavity is independently adjusted with a fine-tuning system to ensure operation in the $\pi/2$ mode.

SIMULATIONS RESULTS

Radio-Frequency Modeling

COMSOL Multiphysics® software [6] is used to compute the electromagnetic field map. The cavity geometry is presented in Fig. 2, where the electric field distribution of the $\pi/2$ mode is illustrated with field lines. The highest electric field is concentrated at the nose region, and there is no field in the coupling cell cavity. The structure aperture is fixed at 3.5 mm.

The on-axis electric field of the 1.8 MeV accelerating structure is represented in Fig. 3. The first four cavities operate as a buncher, the RF window is located on the sixth cavity. The peak gradient along the structure remains uniform, with a maximum peak value reaching 41 MV/m for a peak RF input power of 0.9 MW, compatible with the available magnetron.

The coupling slot between the RF window and the accelerating structure is design to achieve a coupling coefficient β in the range of 1.2 to 1.3 (S_{11} between −21 dB and −18 dB). Figure 4 shows that the S_{11} of the $\pi/2$ mode is at −20.3 dB ($\beta = 1.21$). No additional modes are present within the magnetron bandwidth, thereby facilitating a more reliable and stable startup of the accelerator.

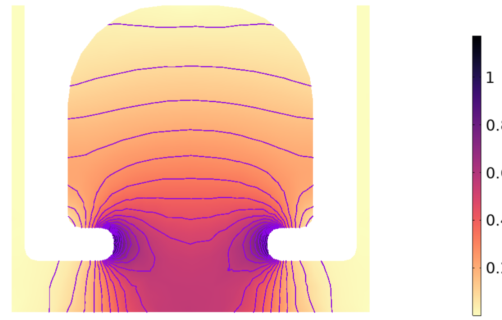

Figure 2: Normalized electric field in accelerating cavity. Iso-value of electric field lines are represented in purple.

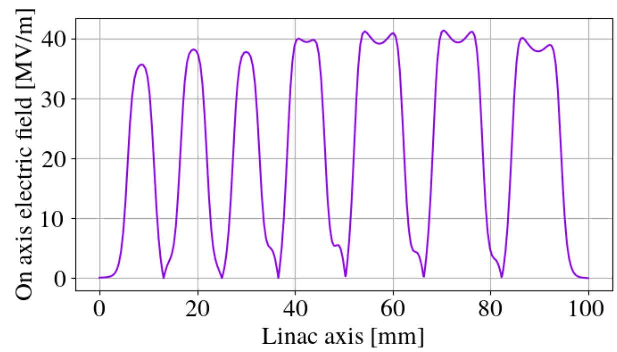

Figure 3: On-axis electric field in the 1.8 MeV accelerating structure.

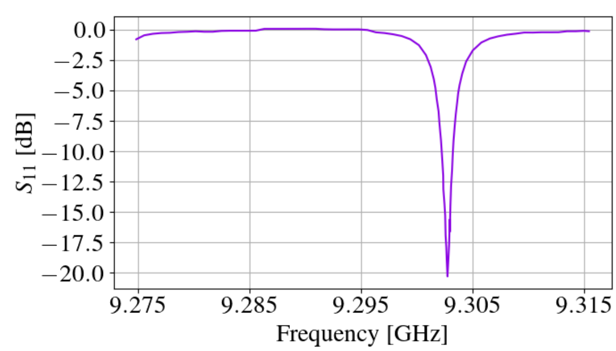

Figure 4: Reflection coefficient S_{11} [dB] of the 1.8 MeV accelerating structure in the bandwidth of the X-band magnetron.

The quality factor of the structure is 8300 and the shunt impedance is 153 MΩ/m. The inter-cell coupling coefficient is 3.8 %.

Beam Dynamics Simulations

Beam dynamics simulations were performed using the particle tracking code RF-Track, developed at CERN [7]. The initial beam parameters were derived from an optical model of the electron gun, corresponding to a 350 mA, 15 keV, converging electron beam.

The energy spectrum is tightly centered around the targeted energy of 1.8 MeV (see Fig. 5). The bunching section has been optimized to reduce the proportion of the low energy particles (below 0.2 MeV). By adjusting the RF power, the accelerator can deliver a clean energy spectrum over a range from 1.6 MeV to 2 MeV, with optimal performance achieved at 1.8 MeV. The output transmission of the structure is 38 % of the initial beam current.

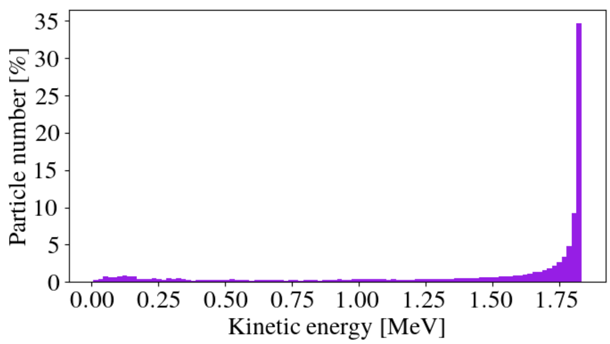

Figure 5: Output energy spectrum of the electrons with 7 cavities.

In Fig. 6 the phase space in the horizontal transverse direction (x) is represented. The FWHM (Full Width Half Maximum) is 0.7 mm, and a similar behavior is observed in the vertical (y) plane. At the end of the accelerating structure, the beam is diverging with 95 % of particles exhibiting a divergence below 15 mrad.

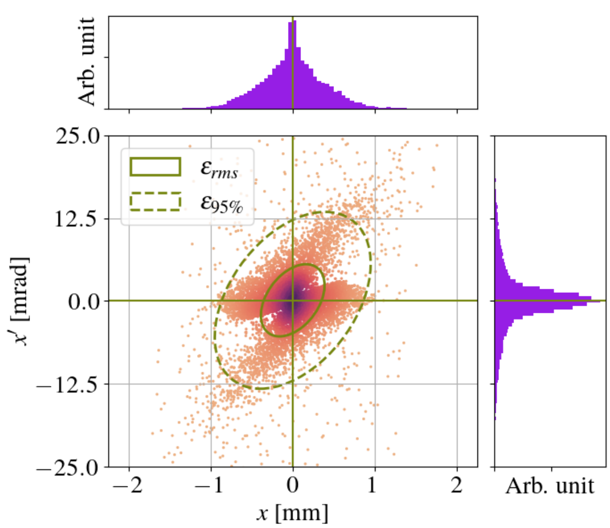

Figure 6: Transverse output phase space of the electrons.

CONCLUSIONS

The RF modeling and beam dynamics simulations have led to a robust design for a compact X-band accelerating structure. All the established specifications are satisfied (see Table 2).

Table 2: Simulation Results of the 1.8 MeV X-band Accelerator

Item	Value	Unit
Energy	1.8	MeV
Length	10	cm
Transmission	38 %	
Quality factor	8300	
Shunt impedance	153	MΩ/m
Frequency	9.3027	GHz
Beam spot size (FWHM)	0.7	mm
On-axis peak gradient	41	MV/m
Peak RF input power	0.9	MW

The manufacturing of the resonant cavities is currently underway. The validation of the whole design, which includes cell coupling, tuning system, and RF coupling will be carried out in the coming months with low-power and high-power tests. In parallel, the development of the other key beamline components has begun, notably the electron gun and the conversion target.

ACKNOWLEDGEMENTS

The authors would like to thank N. Tannoury and T. Campanella for technical supervision and wise advice, R. Convers and V. Parga for mechanical conception, C. Piatkowski for expertise in design of experiments and A. Latina for help with RF-Track.

REFERENCES

[1] Joint Statement on Strengthening the Security of High Activity Sealed Radioactive Sources, IAEA Information Circular, INFCRC/910, Vienna, Austria, 2016, `https://www.iaea.org/publications/documents/infcircs/number/910`.

[2] W.A. Reed, "Chapter 7: Nondestructive Testing and Inspection using Electron LINACs", in *Industrial Accelerators and Their Applications*, R.W. Hamm and M.E. Hamm, R&M Technical Enterprises, Ed. California, USA, 2012, pp. 307-369.

[3] Radiation Source Use and Replacement: Abbreviated Version, National Research Council, USA, 2008, `doi:10.17226/11976`.

[4] R.B. Neal *et al*, "Chapter 6: Design, Fabrication, Installation and Performance of the Accelerator Structure", in *The Stanford Two-Mile Accelerator*, W.A. Benjamin, Inc., New York, USA, 1968, pp.95-162.

[5] Y. Rozier, M. Boucard, "Modelling and Experimental Studies of a X-Band Window for Mobile Linacs", presented at the 17th International Particle Accelerator Conf. (IPAC'26), Deauville, France, May 2026, paper MOP7150, this conference.

[6] COMSOL Multiphysics® v. 6.4. `www.comsol.com`.

[7] *RF-Track Reference Manual*, A. Latina, CERN, Geneva, Switzerland, 2024, `doi:10.5281/zenodo.3887085`.